

Available online at www.sciencedirect.com

jmr&t
Journal of Materials Research and Technology
www.jmrt.com.br



Original Article

Comparison of transformations with inhomogeneous nucleation and transformations with inhomogeneous growth velocity

Mariana Sizenando Lyrio*, André Luiz Moraes Alves, Gabriella Maria Silveira de Sá, Harison da Silva Ventura, Wesley Luiz da Silva Assis, Paulo Rangel Rios

Universidade Federal Fluminense, Escola de Engenharia Industrial Metalúrgica de Volta Redonda, Av. dos Trabalhadores, 420, Volta Redonda, RJ, 27255-125, Brasil

ARTICLE INFO

Article history:

Received 25 April 2019

Accepted 8 August 2019

Available online 31 August 2019

Keywords:

Computer simulation

Microstructure

Phase transformations

Nucleation and growth

transformations

Analytical methods

ABSTRACT

In this paper, we carry out computer simulations of transformations to compare two distinct situations regarding nucleation and growth. The first situation is that in which the nucleation is not homogeneous in space: the nuclei are located inhomogeneously within the matrix, but the growth velocity is the same everywhere. The second situation is that the nuclei are located homogeneously within the matrix, but the growth velocity is inhomogeneous. Microstructure and transformation kinetics of the two transformations are compared. The main result is that the transformation kinetics is affected by either inhomogeneous nucleation or inhomogeneous growth. Nonetheless, an inhomogeneity in nucleation appears to have a stronger effect on the microstructural inhomogeneity than an inhomogeneity in velocity.

© 2019 The Authors. Published by Elsevier B.V. This is an open access article under the CC BY-NC-ND license (<http://creativecommons.org/licenses/by-nc-nd/4.0/>).

1. Introduction

Nucleation and growth transformations are prevalent among solid-state transformations. One way to model these reactions is by using the approach proposed by Johnson-Mehl, Avrami, and Kolmogorov [1–3], the so-called JMAK theory. Instead of modeling the details of the nucleation and growth mechanism JMAK theory prescribed the nucleation rate, the spatial position of the nuclei as well as the growth velocity.

In their original work, they obtained two fundamental and mathematically exact expressions. In both cases, the nuclei

were uniform randomly distributed in space, and the velocity was a constant both in time and space. In the first case, the nucleation proceeded with a constant nucleation rate. In the second case, nucleation sites saturated early in the transformation so that all nuclei were already present at the beginning of the reaction so that only growth would take place. This second case is called “site-saturated,” which we will focus on this work.

Many authors subsequently extended the early work of JMAK. A full account of those extensions is beyond the scope of this paper. Rios and Villa [4–6] give a brief account of these extensions.

Two of those extensions of JMAK are relevant here. In the first, Rios and Villa [4] revisited JMAK theory using modern mathematical tools from stochastic geometry and generalized

* Corresponding author.

E-mail: mlyrio@id.uff.br (M.S. Lyrio).

<https://doi.org/10.1016/j.jmrt.2019.08.012>

2238-7854/© 2019 The Authors. Published by Elsevier B.V. This is an open access article under the CC BY-NC-ND license (<http://creativecommons.org/licenses/by-nc-nd/4.0/>).

JMAK for the situation in which the nuclei density depends on the spatial position of the nuclei, in other words, the spatial distribution of nuclei is inhomogeneous. In the second extension, Villa and Rios [6] proposed a simplified method to extend JMAK for the case in which the growth velocity was position-dependent. The following section contains both analytical results for readers' convenience.

As important as it is to have an accurate analytical description of the transformation, such analytical descriptions have certain practical limitations. The most glaring shortcomings of analytical descriptions are that they deal with mean values, and more importantly, they cannot depict the microstructure. Therefore, the combination of computer simulation and analytical description can be a useful and powerful tool to understand microstructural evolution. Computer simulation can generate the microstructures as a function of time as well as permit the investigation of situations for which there is no analytical description.

In this work computer simulation combined with previously obtained analytical results are used to compare transformations with inhomogeneous nucleation and transformations with inhomogeneous growth velocity.

2. Analytical description of inhomogeneous nucleation and position-dependent velocity

Rios and Villa derived an expression to describe the kinetics of a transformation in which the nucleation sites were located in space according to an inhomogeneous Poisson point process [4]:

$$V_V(t, x) = 1 - \exp\left(-\frac{4\pi}{3} \lambda(x) G^3 t^3\right) \tag{1}$$

Where $V_V(t, x)$ is a time and position dependent mean volume density; $\lambda(x)$ is the intensity of an inhomogeneous Poisson point process. $V_V(t, x)$ reduces to the more usual volume fraction and $\lambda(x)$ reduces to the number of nuclei per unit of volume when λ does not depend on the position. That is the nuclei are located within the matrix according to a homogeneous Poisson point process or less precisely nuclei are uniform randomly located within the matrix. G is a constant growth velocity and t is time. In this work, we restrict this study to the case in which $\lambda(x)$ varies along a single direction. A cellular automata simulation was carried out that investigated inhomogeneous nucleation only [7].

An expression for a position-dependent velocity is more complicated than the expression for inhomogeneous nucleation [6,8]. However, Villa and Rios [6] proposed a simplified approach. In this simplified approach, the growth velocity of each region was constant but depended on the coordinate of the nuclei from which the growth started. That is $G(x)$ depends on the position of the nuclei in space but remains constant upon further growth so that the growing region remains spherical. In the present work, we used a position-dependent/inhomogeneous growth velocity but kept the nucleation homogeneous. Even with the simplifications,

the mathematical expression given by Villa and Rios [6] is more complicated than the one for inhomogeneous nucleation:

$$V_V(t, x) = 1 - \exp(-\lambda \times \text{vol}(A)) \tag{2}$$

$\text{vol}(A)$ is the volume of a set A , the causal cone [6], given by

$$A = \left\{ (y_1, y_2, y_3) \in \mathbb{R}^3 : G(y) t \geq \sqrt{(y_1 - x_1)^2 + (y_2 - x_2)^2 + (y_3 - x_3)^2} \right\} \tag{3}$$

where λ for homogeneous nucleation is equal to the number of nuclei per unit of volume and $G(y)$ is the growth velocity of a region nucleated at $y = (y_1, y_2, y_3)$. (x_1, x_2, x_3) are the coordinates of points in space that satisfy the inequality above. Details can be found in Villa and Rios [6].

An example of a situation in which nuclei density and growth velocity change along one axis is that of a cold-rolled plate in which there is a gradient of deformation across its thickness. Namely, a high deformation/reduction, say 90%, at the top and low deformation at the bottom, say 10%. In terms of this example, here we are going to model and compare only the two extreme and simplest cases: a) the nuclei density changes along the plate thickness, but the growth velocity is the same from top to bottom; b) the nuclei density is uniform across the thickness, but the growth velocity varies from top to bottom. In this way, we can compare the independent effect of inhomogeneous nucleation and position-dependent growth velocity. A more general approach would be to consider both the variation of nuclei density and velocity at the same time. Such a general calculation is significantly more demanding both in terms of computer simulation and analytical description and is currently under investigation.

3. Computer simulation methodology

Computer simulation of the 3D nucleation and growth transformation was carried out using the causal cone method [5,9]. In all cases, nucleation was site-saturated. The matrix comprised $300 \times 300 \times 300$ cubic cells. The dimensions of the simulation volume, henceforward called "the specimen," were taken to be equal to one. Namely, a cube of $[0,1] \times [0,1] \times [0,1]$ corresponding to the axes (x_1, x_2, x_3) . Here we focus on the case in which the total number of nuclei is equal to 300 [10]. At the "bottom" of the simulation volume $x_1 = 0$ whereas at the "top" $x_1 = 1$, as indicated in Figs. 3 and 4, see below. Periodic boundary conditions were adopted except along the x_1 direction. For inhomogeneous nucleation, the nuclei density was supposed to vary linearly along the x_1 direction according to $\lambda(x_1) = mx_1 + n$ where m and n are constants and equal to 596 and 2 respectively [7]. The inhomogeneous growth velocity was supposed to vary linearly along the x direction according to $G(x_1) = ax_1 + b$ where a and b are constants and equal to 3.0 and 0.2, respectively.

4. Kinetics

Figs. 1 and 2 show the transformation kinetics, mean volume density against time, for inhomogeneous nucleation and

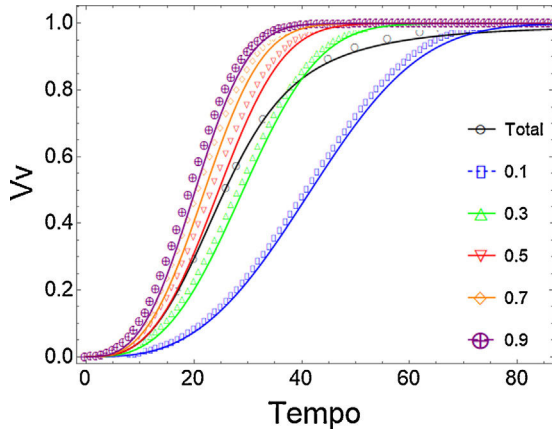


Fig. 1 – Transformation kinetics for inhomogeneous nucleation and homogeneous growth velocity. The transformation kinetics, the mean volume density against time, is slower at the bottom that has a smaller nuclei density than at the top that has a high nuclei density. The solid lines represent the analytical results. The dots represent the simulated data.

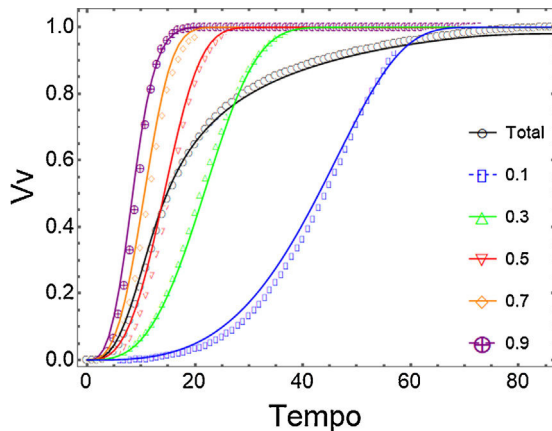


Fig. 2 – Transformation kinetics for homogeneous nucleation and inhomogeneous growth velocity. The transformation kinetics, the mean volume density against time, is slower at the bottom that has a smaller growth velocity than at the top that has a high growth velocity. The solid lines represent the analytical results. The dots represent the simulated data.

inhomogeneous growth velocity, respectively. The total number of nucleation sites is the same in all cases implying that the mean grain volume is the same. The coordinate $x_1 = 0$ corresponds to the “bottom” of the simulation volume, i. e. the “specimen” whereas $x_1 = 1$ corresponds to the “top” of the specimen. Each curve corresponds to the kinetics at a certain point in the sample between $x_1 = 0$ and $x_1 = 1$. Therefore, a plane with $x_1 = 0.9$ is close to the top, whereas a plane with $x_1 = 0.1$ is close to the bottom. The kinetics, i. e. the mean volume density against time, is slower at the bottom than at the top both in Figs. 1 and 2. Therefore, a nuclei density gradient and a growth velocity have similar kinetics. The analytical expressions, Eqs. 1 and 2, describe the curves well [4,6].

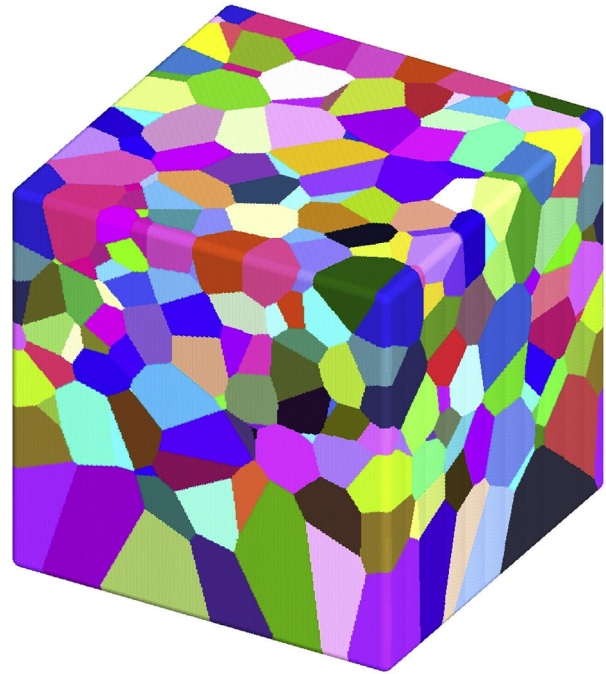


Fig. 3 – 3D representation showing the simulated microstructure with inhomogeneous nucleation and homogeneous growth velocity. The nuclei density was higher at the top of the specimen. As a result, the final grain size is smaller at the top than at the bottom.

Visual inspection of the curves in Figs. 1 and 2 do not allow one to conclude that the slower kinetics was a consequence of either a nuclei density or a growth velocity gradient. The microstructure, Figs. 3 and 4 clarify what is happening.

5. Microstructure

5.1. Inhomogeneous nucleation with homogeneous velocity

Fig. 3 shows a 3D representation of the fully transformed microstructure for inhomogeneous nucleation with homogeneous velocity.

Visual inspection shows that at the top grains are smaller than grains at the bottom. This microstructural gradient is a clear consequence of the nuclei gradient: more nuclei at the top result in small grains, whereas fewer nuclei at the bottom result in larger grains. This result is like that obtained previously by Rios et al. using cellular automata [7]. Therefore, in this case, the interpretation of the microstructure is straightforward and relatively easy to understand.

Another interesting point is that the interfaces between the grains in the fully transformed microstructure are straight lines in 2D and planes in 3D. It is well-known that for homogeneous site-saturated nucleation and constant velocity, the grain boundaries are planes. The resultant grains form a Poisson–Voronoi tessellation. The straight boundaries are also seen here showing that even for site-saturated inhomogeneous nucleation the characteristic of the homogeneous nucleation persists.

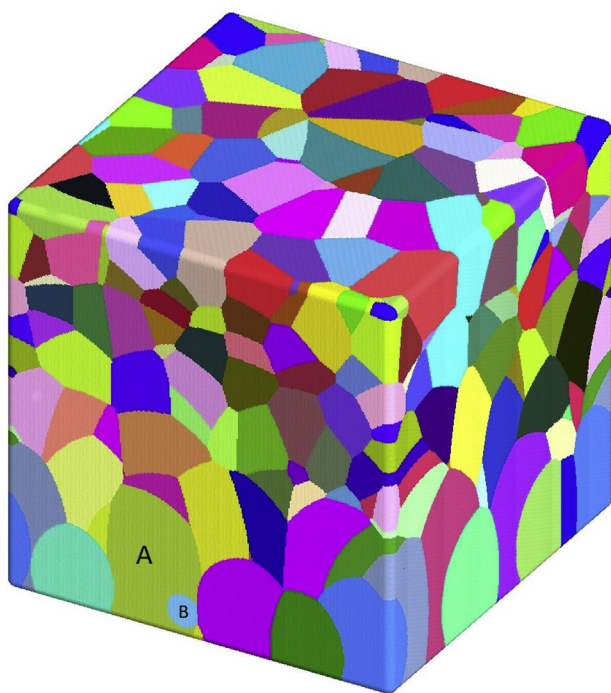


Fig. 4 – 3D representation showing the simulated microstructure with homogeneous nucleation and inhomogeneous growth velocity. The growth velocity was higher at the top of the specimen. As a result, the final grain size is smaller at the top than at the bottom.

5.2. Inhomogeneous velocity with homogeneous nucleation

Fig. 4 shows a 3D representation of the fully transformed microstructure for inhomogeneous velocity with homogeneous nucleation.

Visual inspection shows that at the top grains are smaller than grains at the bottom. This microstructural gradient is a consequence of the velocity gradient: faster growth at the top result in smaller grains than the slower growth at the bottom.

A gradient in velocity also produces a microstructural gradient. It is difficult to compare the effect of a gradient of nuclei with that of a gradient in velocity on the microstructural inhomogeneity. Such a comparison is difficult because we would be comparing different things. Nonetheless, in addition to the simulations show here, we performed a considerable number of simulations changing the number of nuclei and the gradients. These are not shown here for reasons of space. All this allowed us to tentatively say that inhomogeneous velocity is less effective in producing a microstructural gradient than inhomogeneous nucleation. We discuss this point in more detail later in this paper.

Another exciting feature of Fig. 4 is that the grain boundaries are curved in contrast to the boundaries shown in Fig. 3 that are straight. The boundaries are curved because of the inhomogeneous velocity. A fast-growing grain tends to “go around” a slower-growing grain. As a result, the boundary of the fast grains is concave, whereas the boundary of the slower grain is convex [11]. One can use this difference as a

“metallographic pointer” to distinguish between the two cases simulated here.

6. Discussion

The problem of an inhomogeneous velocity is far more complicated than the issue of inhomogeneous nucleation. Even computer programming presents more difficulties in the case of inhomogeneous velocity than in the case of inhomogeneous nucleation. For inhomogeneous velocity, one must control at every step if a certain point is being transformed by a fast-growing grain that is farther from this point or by a slower-growing grain that is closer.

The microstructural inhomogeneity produced by an inhomogeneous velocity depends on the number of nuclei not only on the gradient itself. A thought experiment might clarify this point.

Consider a situation when one has only two nuclei one set at $x_1 = 0.75$ and another set at $x_1 = 0.25$ along the central axis of the specimen. Suppose that the growth velocity of the $x_1 = 0.75$ nucleus is 3 times the growth velocity of the $x_1 = 0.25$ nucleus. Thus, the grain resulting from the $x_1 = 0.75$ nucleus will be much larger than the grain resulting from the $x_1 = 0.25$ nucleus.

Consider now another situation when one has three nuclei one set at $x_1 = 0.75$, another set at $x_1 = 0.5$, and another set at $x_1 = 0.25$ along the central axis of the specimen. Suppose that the growth velocity of the $x_1 = 0.75$ nucleus is 3 times the growth velocity of the $x_1 = 0.25$ nucleus. Suppose also that the growth velocity of the $x_1 = 0.5$ nucleus is twice the growth velocity of the $x_1 = 0.25$ nucleus. In this situation, the presence of the $x_1 = 0.5$ nucleus will prevent the growth of the $x_1 = 0.75$. Consequently, the grain resulting from the $x_1 = 0.75$ nucleus will not be so much larger than the grain resulting from the $x_1 = 0.25$ nucleus as in the previous case. In other words, the microstructural inhomogeneity will be less severe. One can continue to add nuclei, say between $x_1 = 0.75$ and $x_1 = 0.5$ that will further limit the growth of the region resulting from the $x_1 = 0.75$ nucleus.

Fig. 4 provides an illustration of a grain growing fast and outgrowing a grain with a slower velocity. The grain marked “A” grows faster than the grain marked “B” because of the velocity gradient. It grows down to the bottom and limits the growth of grain “B.” This kind of behavior is the basis for a velocity gradient producing an inhomogeneous microstructure.

Nonetheless, with 300 nuclei, one could not detect a significant effect of the velocity on the grain size along with x_1 . The grain size measured on the planes ranging from $x_1 = 0.1$ to $x_1 = 0.9$ remained roughly the same.

7. Summary and conclusions

In this work, computer simulation and analytical models were used to compare the effect of an inhomogeneous nuclei density with an inhomogeneous growth velocity. The main conclusions are:

- All computer simulations showed good agreement with the analytical model of Rios and Villa [4,6].
- The transformation kinetics of an inhomogeneous nuclei density and an inhomogeneous growth velocity are similar.
- The microstructures of both inhomogeneous nucleation and inhomogeneous growth velocity are inhomogeneous.
- However, inhomogeneous growth velocity appears to be less capable of promoting a microstructural inhomogeneity than inhomogeneous nucleation.
- Moreover, an inhomogeneous growth velocity produces curved grain boundaries, whereas a constant growth velocity with inhomogeneous nucleation yields straight grain boundaries.

Conflicts of interest

The authors declare no conflicts of interest.

Acknowledgments

This study was financed in part by the Coordenação de Aperfeiçoamento de Pessoal de Nível Superior - Brasil (CAPES) - Finance Code 001. The authors are grateful to Conselho Nacional de Desenvolvimento Científico e Tecnológico, CNPQ and Fundação de Amparo à Pesquisa do Estado do Rio de Janeiro, FAPERJ, for the financial support.

REFERENCES

- [1] Johnson WA, Mehl RF. Reaction kinetics in processes of nucleation and growth. *Trans AIME* 1939;135:416-41.
- [2] Avrami MJ. Kinetics of phase change I general theory. *J Chem Phys* 1939;7(12):1103-12.
- [3] Kolmogorov NA. The statistics of crystal growth in metals. *Isvestiia Akademii Nauk SSSR - Seria Matematicheskaja* 1937;1:333-59.
- [4] Rios PR, Villa E. Transformation kinetics for inhomogeneous nucleation. *Acta Mater* 2009;57:1199-208.
- [5] Rios PR, Villa E. Application of stochastic geometry to nucleation and growth transformations. In: Molodov DA, editor. *Microstructural design of advanced engineering materials*. 1st ed. Weinheim, Germany: Wiley-VCH; 2013. p. 119-59.
- [6] Villa E, Rios PR. On modelling recrystallization processes with random growth velocities of the grains in materials science. *Image Anal Stereol* 2012;31:149-62.
- [7] Rios PR, Jardim D, Assis WLS, Salazar TC, Villa E. Inhomogeneous Poisson point process nucleation: comparison of analytical solution with cellular automata simulation. *Mater Res* 2009;12:219-24.
- [8] Capasso V, Burger M, Micheletti A, Salani C. Mathematical models for polymer crystallization processes. In: Capasso V, editor. *Mathematical modelling for polymer processing. Mathematics in Industry 2*. Berlin Heidelberg: Springer-Verlag; 2003. p. 167-242.
- [9] Cahn JW. The Time Cone Method for Nucleation and Growth Kinetics on a Finite Domain. *Mater Res Soc Symp - Proc* 1996;398:425-37.
- [10] Da Costa MFB. Simulação computacional de transformações não homogêneas por nucleação e crescimento. [M. Sc. Dissertation]. Universidade Federal Fluminense (Escola de Engenharia Industrial Metalúrgica de Volta Redonda); 2017.
- [11] Alves ALM, Assis WLS, Rios PR. Computer simulation of sequential transformations. *Acta Mater* 2017;126:451-68.